ICMIEE-PI-140424

Fracture Properties of Graphene Oxide (GO) and GO/CNT Hybrid papers

Md. Nizam Uddin [1] *& Jang-Kyo Kim* [2]
[1] Department of Mechanical Engineering, Khulna University of Engineering and Technology (KUET), Khulna-9203, Bangladesh
[2] Department of Mechanical and Aerospace Engineering, The Hong Kong University of Science and Technology, Clear Water Bay, Kowloon, Hong Kong

Email address: engrnizam02@gmail.com

Abstract
The fracture behaviors of graphene oxide (GO) and GO/multi-walled carbon nanotube (MWCNT) hybrid papers are studied in mode-I and mode-III fracture. The effects of GO sheet size and CNT content on fracture and tearing toughness of the papers are evaluated using double-edge-notch tension (DENT) and trouser tear specimens, respectively. The tearing studies of all paper specimens under mode-III loading exhibited stick-slip tearing. The concept of Linear Elastic fracture mechanics (LEFM) is used to measure the fracture toughness of GO and bucky papers and GO/CNT hybrid papers. Large GO papers give rise to a higher energy release rate and tearing toughness than those made from small GO sheets: about 36% and 70% enhancements are shown for the large GO papers due to a more compact structure and better GO sheet alignment. Hybridization of GO papers with MWCNTs also improves these properties when up to 5 wt.% of MWCNTs is incorporated, attributed to the stronger GO interlayer bonds through pi-pi interactions with intercalated MWCNTs. Fracture surface examination indicates that cleavage failure prevails in mode-I fracture depending on the size of GO sheets: the unsorted and large GO papers fail mainly by brittle cleavage of GO sheets whereas small GO papers fail by combined brittle cleavage and minor pullout following de-bonding of GO bundles. In contrast, combination of cleavage and de-bonding failures is dominant in mode-III fracture of GO papers, regardless of GO size. CNT pullout is the dominant failure mechanism in both fracture modes of bucky papers.

Keywords: Graphene oxide paper, Fracture toughness, Energy release rate, Cleavage failure, Vacuum filtration.

1. Introduction
Since its discovery in 2004 [1], graphene - the parents of all graphitic materials has become one of the most exciting topics of research in the last few years. Graphene consists of one atom thick sp^2 bonded carbon atoms arranged in a honeycomb lattice structure, and possesses exceptionally high in-plane electronic mobility, mechanical properties and thermal/electrical conductivities [2, 3]. Among different methods for the fabrication of graphene based materials, graphene oxide (GO) synthesized from oxidation of graphite is the most versatile method [4]. GO is an atom thick sheet of graphite containing oxygenated functional groups on its basal plane and at its edges, which form a hybrid structure of sp^2 and sp^3 hybridized carbon atoms, making it dispersible in water and organic solvents [5].GO has been widely used as a building block in composites, mechanical actuators, nano-robots, energy related materials, biological and medical applications [6, 7]. In recent years, GO-based paper materials have attracted much interest because of their outstanding strength, modulus and high degree of flexibility [8]. These paper-like materials may be used as sealants, actuators, bio-compatible substrates, flexible substrates and super-capacitors with high chemical and thermal stability [9]. GO papers can be easily fabricated from aqueous GO dispersion via vacuum-assisted self-assembly to form a free standing layer-by-layer hierarchical structure.

The mechanical properties of GO papers have been extensively studied mainly in unidirectional tensile and bending modes [10, 11]. GO papers had a high strength and modulus in tension and bending due to the interlocking-tile microstructure of individual GO nano-sheets in the paper. Earlier studies indicate that these properties of GO papers outperformed other paper-like materials [12] while being similar to those of flexible graphite foils and carbon nanotube (CNT) bucky papers [11]. However, depending on a number of factors, including the precursor materials and how they are produced, the measured properties differed considerably, e.g. the tensile strength varied between 76 and 293MPa and the moduli between 6 and 42

GPa [13]. Significant efforts have been directed towards improving the mechanical properties of GO papers, mainly by intercalation of polymer layers and chemical cross-linking between the GO sheets. These techniques include intercalation of divalent ions, such as Mg^{+2} or Ca^{+2} [12], polyvinyl alcohol films [14, 15], octadecyclamine (ODA) [10], polydopamine (pDOP) [16] and the combination of pDOP and polyetherimide (PEI) [13]. The mechanical properties of GO papers have been extensively studied mostly in uni-axial tensile mode [17-19]. While very few studies have been reported on the properties of GO paper in other modes of deformation, such as in shear or tearing. The lateral dimensions of GO sheets have significant impacts in controlling the properties and application of GO papers. Large and small GO sheets, respectively, are ideally suited in a variety of applications. For example, polymer-based composites containing small GO sheets are useful for bio-sensing and drug delivery [20, 21], whereas large GO sheets with controlled sizes are preferable for optoelectronic devices [22, 23].Various methods have been proposed to control the GO size or to obtain large sizes with varied successes [24-26], including the use of less oxidation and sonication. In this study, a series of centrifugation was used to sort as-produced GO sheets into different size groups based on our previous study [23]. Like GO papers, papers made from CNTs is a viable engineering material due to their useful mechanical, electrical and thermal properties. They are used in applications, like actuators, capacitors, electrodes, field emission devices, radio frequency filters, artificial muscles and strain sensing [27, 28].CNTs were also combined with GO sheets to synthesize hybrid papers in this study. This works aims the evaluation of the fracture resistance and identifying the corresponding failure mechanisms of neat GO and hybrid papers in two different modes, including mode I fracture using the double edge notched tensile (DENT) test and mode III tearing using the trouser test. Experiments were performed to determine the fracture and tearing toughness of GO papers and GO/CNT hybrid papers. In addition, the study specially focuses on the effects of GO sheet size and CNT content on the fracture properties of these papers were specifically studied.

2. Experimental

2.1 Fabrication of GO and GO/CNT hybrid papers

GO was prepared from purified natural graphite flakes (Asbury Graphite Mills) based on modified chemical method [29, 30] and the procedure for GO synthesized is described elsewhere [23, 31]. GO paper was fabricated by flow-directed vacuum filtration of aqueous GO dispersions through a Millipore filter membrane (90 mm in diameter and 0.22 μm pore size) followed by air drying and peeling off from the filter paper. The thickness of each paper is controlled by adjusting volume of the aqueous GO dispersions. For the fracture toughness testing specimen, the thickness of the paper was about 20±0.001μm. All the specimens were dried in an oven at 60°C for seven days to achieve low moisture content before testing. To investigate the effect of GO sheet size on the fracture properties the as prepared unsorted GO solution was separated into 'small GO' and "large GO" through three-step centrifugation on a table-top centrifuge (SIGMA 2-16P) whose average areas were 1.1 and 272μm^2, respectively [32]. Raman spectroscopy (Renishaw MicroRaman/Photoluminescence System with a 633 nm He-Ne laser) and **X**-ray diffraction (XRD, X'pert Pro, PANalytical, using Cu Kα1 (λ =0.154 nm) radiation) analysis were used to evaluate the carbon structure and the interlayer distance between adjacent GO layers with different size groups. For the GO/CNT hybrid paper fabrication, the functionalized CNTs solutions were poured into GO aqueous dispersion while stirring followed by 0.5 hr ultrasonication. The GO/CNT hybrid paper was prepared by vacuum filtration of GO/CNT hybrid mixture followed by air drying and peeling from the filter paper and finally dried in a vacuum oven at 60°C. The CNT content was varied between 2.5 and 90 wt%.

2.2 Fracture toughness tests and characterization

The fracture resistance of papers was characterized both in mode I tension using the double edge notched tension (DENT) test and in mode III out-of-plane shear using the trouser tear test. The specimens were prepared according to the specifications ASTM E399 and ASTM D1938, respectively, and their dimensions are as shown in Fig. 1. For the DENT specimens, the width, *2b*, was varied between 5 and 30mm while the crack length to width ratio, *a/b*, was varied between 0.15 and 0.69. The critical stress intensity factor, K_{IC}, was calculated using the equations (1) and (2) when the external stress reached a critical value, σ_c, for crack propagation [33]:

$$K_C = \sigma_C\sqrt{\pi a}\ F\left(a/b\right) \quad (1)$$

Where $F\left(a/b\right)$ is a geometric correction factor and for a double edge notch tension specimen is given:

$$F\left(a/b\right) = 1.12 + 0.203\left(a/b\right) - 1.197\left(a/b\right)^2 + 1.93\left(a/b\right)^3 \quad (2)$$

The mode-I stress intensity factor, K_C, is related to the energy release rate, G_C, by

$$G_C = \frac{K_C{}^2}{E} \qquad (3)$$

Where E is the Young's modulus of the material for plain stress condition

For the trouser tear test specimens, two different ligament lengths of 30 and 50mm were employed while the initial crack length was fixed at 15 mm. The tearing toughness, G, was calculated by:

$$G = {}^{2F}/_{t} \qquad (4)$$

Where F is the mean force calculated by averaging the load over the entire ligament length; and t is the thickness of the specimen. Thus, the tearing toughness is the internal tearing resistance and measures the force perpendicular to the plane of the paper necessary to tear a single sheet through a specified distance after the tear has already been started. Specimens were cut to the dimensions shown in Fig. 2 and the initial cracks were made using a sharp surgical blade. The specimens were dried in an oven at 60°C for seven days to uniformly dry before testing. The DENT and trouser tear tests were conducted on a universal testing machine (Alliance RT/5) at cross-head speeds of 1 and 250 mm/min, respectively, according to the specifications. The fracture surface morphologies were examined on a scanning electron microscope (SEM, JEOL 6700F, JSM) and an optical microscope (LEICA M205C).

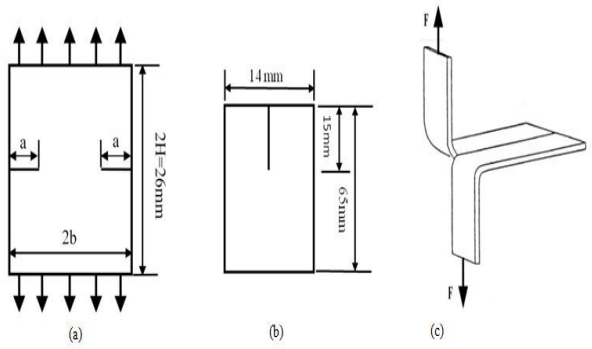

Figure 1. (a) Double edge notched tension specimen and (b) Trousers tear specimen and (c) model geometry (tearing test).

3. Results and Discussion

3.1. Materials Characteristics

Fig.2a. shows the Raman spectra of small, unsorted and large GO papers and the corresponding I_D/I_G intensity ratio. The G band (at ~1590 cm^{-1}) is Raman active for sp^2-hybridized carbon-carbon bonds in graphene [34, 35] while D band (at ~1354 cm^{-1}) is associated with the presence of defects in the graphite material such as bond-angle disorder, bond-length disorder, vacancies, edge defects, etc. [36]. The intensity ratio I_D/I_G is widely used to measure the defects quantity in graphitic materials [37].The Raman spectra shows an increase in the D/G intensity ratio from 2.02 for large GO to 2.43 for small GO, clearly indicate the increased defects quantity in small GO sheets for a given area of materials.

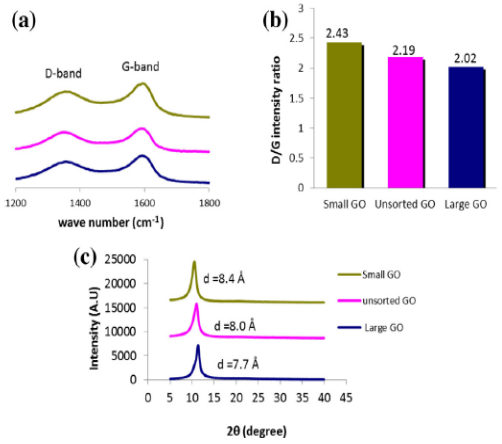

Figure 2. Raman spectra of small, unsorted and large GO papers (a) D- and G-band peaks; (b) I_D/I_G intensity ratio and (c) X-ray diffraction patterns of small, unsorted and large GO papers.

The XRD pattern (Fig.2c) of small, unsorted and large GO papers exhibits a characteristic XRD peak at 2θ = 10.53°, 11.03°, 11.35° and corresponding to a distance of, 8.4 Å, 8.0 Å and 7.7Å between the stacked GO sheets. The larger was the GO sheets, the smaller was the d-spacing. This observation is consistent with the Raman intensity ratio, where the large GO sheets contained fewer oxygenated functional groups for a given area, leading to a shorter distance between them. In other words, the large GO papers had a more compact structure and better GO sheet alignment formed during the self-assembly process than the small GO papers [32].

3.2. Fracture properties of GO papers and GO/CNT hybrid papers

The mode-I strain energy release rates, G_c, were calculated using equation (3) from the Young's moduli of GO papers determined by the dynamic mechanical analysis**.** The results on the effects of initial crack length and specimen width are shown in Fig. 3. The strain energy release rate showed a maximum value of ~0.34 kJ/m^2 for a/b in the range of 0.38 to 0.46, and decreased gradually when a/b ratio was reduced or increased. A further study on the effect of specimen width, 2b, indicates that the energy release rate leveled off when 2b reached ~10 mm for both a/b = 0.38 and 0.46.

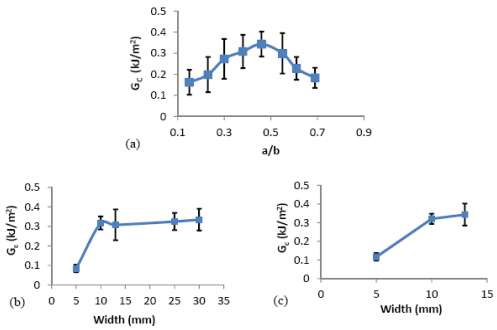

Figure.3- Energy release rates of GO papers: (a) Effect of initial crack length to specimen width, a/b, for a fixed width b = 13mm; Effect of specimen width 2b for a fixed crack length to width ratio (b) a/b = 0.38 and (c) a/b = 0.46

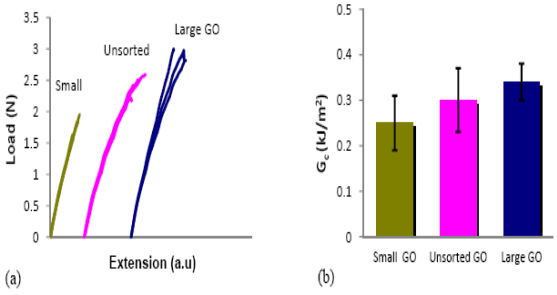

Figure. 4 (a) Load- extension curves and (b) comparison of the strain energy release rates of small GO, unsorted GO and large GO papers, crack length to width ratio a/b = 0.38, width 13mm

As prepared GO sheets were sorted as small GO and large GO sheets and the effect of GO sheets size on fracture properties were investigated. The representative load-extension curves obtained from the fracture toughness tests are shown in Fig.4 (a) and the corresponding strain energy release rates are given in Fig. 4(b). From Fig. 4(a) load increased almost linearly with extension when crack initiated until it reached the maximum where catastrophic failure occur. This indicates that fracture behavior of GO paper is like a brittle material. The energy release rates were higher in the ascending order of small, unsorted and large GO papers, with a significant 36% difference between the small and large GO sheets.

To understand the different fracture behaviors of GO papers made from different size groups, SEM images were taken from the cross-sectional fracture surfaces, as shown in Fig. 5.

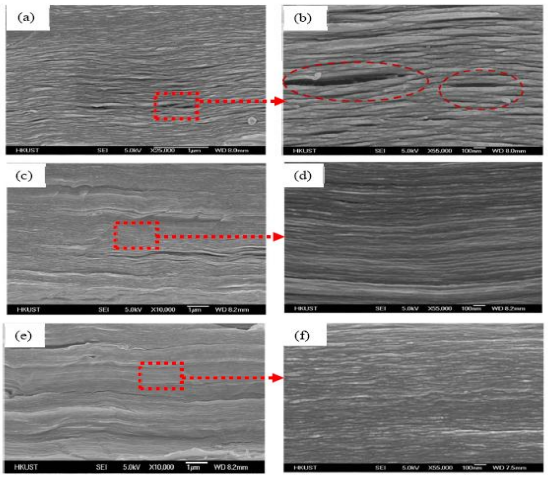

Figure 5. SEM photographs of the fracture surfaces of GO paper (a,b) unsorted GO,(c,d), large GO and (e,f) small GO

GO paper assembled in a layer-by-layer hierarchy where GO sheets are bridged on the edges (intralayer) and adjacent graphene sheets (interlayer) through *sp*2 carbon-carbon covalent bonds, hydrogen bonds, van der Waals forces [32]. When the crack propagated across to the stacked GO sheets, it generally followed a straight path without much deflection. The *sp*2 carbon-carbon covalent bonds are short-ranged and the deformation of GO sheets generally involves the localized processes of bond breaking. [38]. Therefore, all fracture surfaces presented mainly cohesive failure via brittle cleavage of GO sheets with limited GO sheet pullout. However, depending on the GO size group used, the surface morphologies presented obvious differences in term of degree of GO sheet alignment in the horizontal direction and the occurrence of de-bonding between them. It is of interest to note that the large the GO sheets, the better the alignment and the less the tendency to de-bonding. However, the elongated elliptical holes shown in Fig. 5(b) appear to be the trace of de-bonded GO sheets or bundles, consistent with the size of small GO sheets ranging from a few hundred nm to a few μm in lateral

length. In summary, it can be said that the fracture mechanisms of unsorted and large GO papers were dominated by brittle cleavage of GO sheets whereas small GO papers were failed by combined brittle cleavage and minor pullout following de-bonding of GO sheets.

Similar to GO papers, specimens made from CNT papers and the GO/CNT hybrid papers were tested at a/b = 0.38 to measure the fracture toughness. The critical stress intensity ratios, K_c, of GO/CNT hybrid papers are presented as a function of CNT content in Fig. 6(a). (Due to the lack of individual Young's modulus data, the K_c values are shown.) The stress intensity factor of the neat CNT papers was below one tenth that of the neat GO paper (K_c = 0.103 vs 1.5 MPa$\sqrt{m}$) although the strain energy release rate was only five times lower (G_c = 0.072 vs 0.34 kJ/m^2), a reflection of the difference in Young's modulus. The neat CNT papers are a mat of randomly entangled CNTs with a randomly interconnected porous structure. During the filtration process the CNTs were self-assembled by van der Waals forces. The interaction of individual CNT plays an important role in determining the mechanical properties of the bucky paper [39, 40]. When load is applied, individual CNTs began to unravel (disentangle) by tube to tube shearing from each other until a peak load is reached and following this limit, crack propagates across the sample by pullout of the CNTs. The failure mechanism involved complete pullout of the CNTs across the crack (Fig. 6(b)). The fracture toughness of GO/CNT hybrid papers showed an interesting variation with CNT content (Fig. 6(a)).

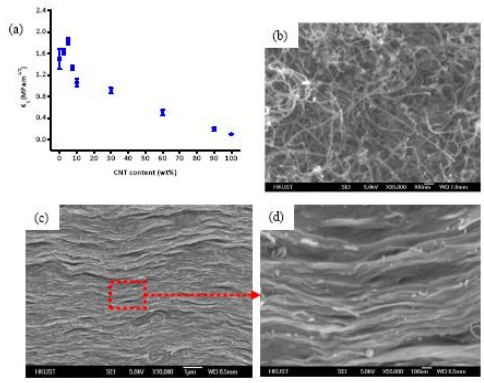

Figure. 6 (a) Fracture toughness of GO/CNT hybrid papers as a function of CNT content; fracture surface morphologies of (b) neat CNT bucky paper and (c, d) 95 wt.% GO/5 wt.% CNT hybrid paper.

It sharply increased for CNT contents up to 5 wt.% before a consistent, parabolic reduction with further increase in CNT content. A small amount of CNTs intercalated between the GO sheets positively contributed to resisting the crack opening force by strongly adhering to the GO sheets via π-π interactions which are considered stronger than the hydrogen bonds or van der Waals forces present between the GO sheets alone. This may explain the initial surge in fracture toughness by 22% with 5 wt.% CNTs. The SEM images corresponding to these papers (Fig. 6(c) and 6(d)) indicate that the fracture mechanisms were largely different from those of the neat GO papers and two distinct features can be identified. There was evidence of GO bundle pullout along with the intercalated CNTs, and as a result the fracture surface was much rougher than the neat GO papers. The bundle pullout mechanism is considered to positively contribute to the toughness of the hybrid papers through crack tip deflection. The addition of a small quantity of CNTs hindered cleavage as well as deboning of GO sheets. Another feature is that the GO sheets were stacked with a high degree of wrinkles in the form of sinusoidal waves along with uniformly intercalated CNTs. The presence of wrinkles may have helped the pullout of GO sheet bundles, which otherwise seldom occurred in well-aligned GO sheets (Figs. 5d, 5f).

However, the excessive amount of CNTs beyond 5 wt.% failed to enhance the fracture toughness because the bonds with the GO sheets were not as strong due to the agglomeration of CNTs, while inevitably increasing the total paper thickness because of the loose packing density of CNTs compared to the neat GO sheets.

3.3. Tearing properties of GO papers and GO/CNT hybrid papers

The out of plane mode-III trouser tear tests were carried out to determine the tearing toughness of papers. The effects of GO sheet size on tearing toughness are shown in Fig. 7. It shows the typical load-extension curves obtained during tear propagation of small, unsorted and large GO papers. From the load extension curves it is observed that force slowly increase to a maximum value and drops rapidly to a minimum value with corresponding variations in the rate of propagation. The crack initiate at maximum force while arrest at minimum force. This type of tearing is called stick-slip tearing. At regular intervals, the crack initiation and arrest repeats itself [41]. The stick-slip tearing has also been observed in thermoplastic elastomers [42, 43] and polyvinyl alcohol gel sheets [44]. As expected, there was a linear increase in tearing toughness with increasing paper thickness (Fig. 7(b)). The effect of GO sheet size on tearing toughness is shown in Fig. 7(c), the large GO papers presenting ~70% enhancement compared to the small GO papers. The

dependence of tearing toughness on GO size is attributed to two interrelated characteristics, namely the compactness of GO paper and the presence of defects in GO sheets. The XRD analysis clearly indicated a shorter interlayer distance between the large GO sheets, i.e. with a more compact structure, than the small sheets, while the large GO sheets contained fewer defects than small GO sheets as indicated by the Raman I_D/I_G intensity ratio (Fig. 2). In fact, the dependency of tearing toughness on GO sheet size has a significant analogy with the dependency of tearing toughness of cellulose papers on fiber length: it was shown that the tearing resistance increased with increasing fiber length, particularly when there was low bonding between the fibers [45].

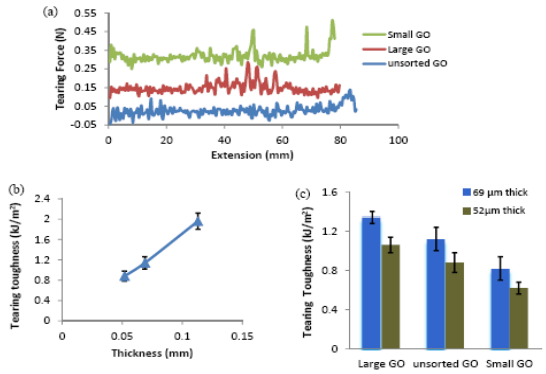

Figure 7. (a) Tearing force-extension curves of 0.052 mm thick GO papers; (b) tearing toughness of unsorted GO papers as a function of specimen thickness; and (c) tearing toughness of GO papers with different size groups.

The degree of bonding in the paper significantly affected the tearing process. In papers with a higher degree of bonding, the fibers were well anchored in the paper and the load during the tear test caused fibers to break [46]. This finding on cellulose papers is also very similar to our observation in GO papers as discussed below. The tearing process in GO papers was complex because the plane of fracture changed during the tear propagation: the fracture surface was initially oriented perpendicular to the paper face and tended to become almost 180° at the end [47], showing large, flat torn surface areas (Figs. 8(a) and 8(c)).On the microscopic scale, the torn fracture surfaces were uneven and irregular: although there were large differences in overall tearing toughness, the torn surface morphologies were in general similar for all GO papers. Essentially, fracture occurred due to the combination of two distinct failure modes, namely cohesive and adhesive failures. Because the cracks always propagate through the weakest paths, there were competitions between the tearing strength of the individual or bundle GO sheets and the force to separate between them, leading to cleavage fracture and de-bonding, respectively, once the driving force overcame each of the resistance. Judging from the lower tearing toughness of the small GO papers than the large GO papers, it is assumed that cleavage was more dominant than the de-bonding mechanism.

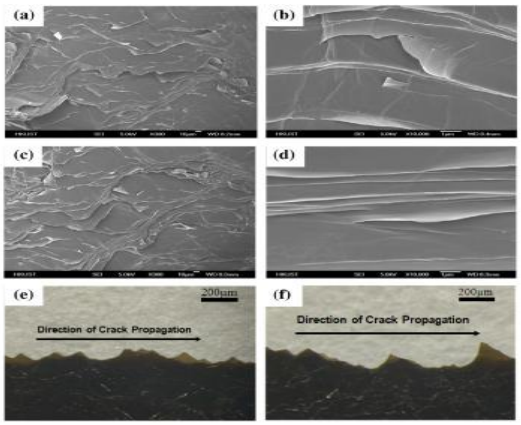

Figure 8. SEM photographs of torn surfaces of (a, b) small GO papers and (c, d) large GO papers; optical images of torn edges of (e) small and (f) large GO papers.

This hypothesis is partly confirmed by the optical images showing twisty crack paths at the edges of the papers (Figs. 8(e) and 8(f)). The torn edges presented typical of a saw tooth wave with disordered oscillation where the large GO papers exhibited generally higher amplitude peaks than the small GO papers, a reflection of inherent GO sheet size. The tearing toughness of GO/CNT hybrid papers is plotted as a function of CNT content as shown in Fig. 9(a). The tearing toughness of the neat CNT paper was only ~3.0% that of neat GO papers (0.033 vs 1.1 kJ/m^2 for 69 μm thick papers), and was even much less than half the mode I fracture toughness (0.072 kJ/m^2) of the same material.

Figure 9. (a) Tearing toughness of GO/CNT hybrid papers as a function of CNT content; typical SEM image of torn surface of GO/CNT hybrid paper with (b) 5 wt.% and (c) 10 wt.% CNTs.

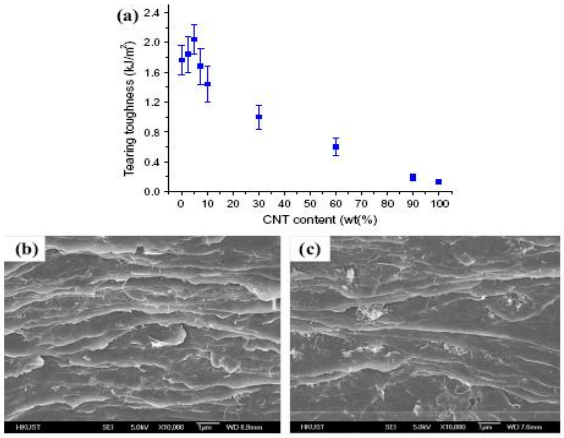

It is assumed that the highly porous structure of CNT papers was less resistance to fracture in out-of-plane shear than in uni-axial tension because the crack propagation occurred mainly by disentanglement of CNT bundles assembled by weak van der Waals forces. The torn fracture surface of the CNT papers had a much the same morphology as for the mode I fracture surface (Fig. 6(b)), indicating CNT pullout was the dominant failure mechanism in tear.

Resembling the mode I fracture toughness values (Fig. 6(a)), the hybrid papers containing a small amount of CNTs showed an ameliorating effect on tearing toughness. With 5 wt.% CNTs, the tearing toughness of the hybrid papers increased by almost 15% compared to the neat GO papers, a manifestation of strong bonds between the CNTs and GO sheets. With further addition of CNTs, the tearing toughness continued to drop, similar to mode I fracture toughness, but above the value corresponding to the neat CNT papers. The torn surface of the GO/CNT hybrid papers produced complex fracture morphologies (Figs. 9(b) and 9(c)) which significantly differ from those of the neat GO papers (Figs. 8(b) and 8(d)), all of whom were taken at a similar magnification. It is interesting to note that the hybrid papers showed generally more GO torn edges than the neat GO papers, perhaps as a result of more uniform dispersion of GO sheets aided by the presence of CNTs. The intercalated, small amount of CNTs enhanced the GO inter sheet bonds through the π-π interactions as discussed above. The CNTs were well dispersed when the CNT content was low (5 wt.%), and with increasing the CNT content (10 wt.%) they tended to be agglomerated, unable to improve the tearing toughness.

4. Conclusions

The fracture resistance of neat GO and GO/CNT hybrid papers was studied and the corresponding failure mechanisms are identified in two different modes, including mode I fracture using the double edge notched tensile (DENT) test and mode III tearing using the trouser test. The effects of GO sheet size and CNT content on the fracture properties of these papers were specifically studied. An easy and efficient centrifugation was used to sort the (as-prepared) GO sheets into two different size groups, large and small GO sheets. The following can be highlighted from the experimental study.

GO paper made from large GO sheet gives higher fracture and tearing toughness than those from small GO sheets. About 36% enhancement of strain energy release rate and 70% enhancement of tearing toughness were observed. Hybridization with CNTs also enhanced these two properties only when small amounts of CNTs were incorporated so as to maintain strong bonds with the surrounding GO sheets: the fracture toughness increased by 22% and tearing toughness by 15% after hybridization with 5 wt.% of CNT, compared to the neat GO papers. The failure mechanisms taking place during the quasi-static fracture and trouser tearing tests were identified from the microscopic examination of the fracture surfaces. Cohesive failure and combination of cohesive/adhesive failures were found in mode-I and mode-III fracture of GO papers, respectively. The torn edges exhibited typical of a saw tooth wave with disordered oscillation where the large GO papers had generally higher amplitude peaks than the small GO papers. In contrast, the GO/CNT hybrid papers failed mainly by a combination of the above mechanisms plus CNT pullout, depending on CNT content.

References

[1] K.S. Novoselov, A.K. Geim, S.V. Morozov, D. Jiang, Y. Zhang, S.V. Dubonos, V. Grigorieva, A.A. Firsov, Electric field effect in atomically thin carbon films, Science, 306, 666-669, 2004.

[2] K.S. Novoselov, A.K. Geim, S.V. Morozov, D. Jiang, M.I. Katsnelson, S.V. Dubonos, A.A. Firsov, Two dimensional gas of mass less dirac fermions in graphene, Nature, 438, 197–200, 2005.

[3] A.K. Geim, K.S. Novoselov, The rise of graphene, Nat. Mater, 6, 183-191, 2007.

[4] W.S. Hummers, R.E. Offeman, Preparation of graphitic oxide, J. Am. Chem. Soc. 80, 1339, 1958.

[5] S. Stankovich, R. Piner, S.T. Nguyen, R.S. Ruoff, Synthesis and exfoliation of isocyanate-treated graphene oxide nanoplatelets, Carbon, 44, 3342–3347, 2006.

[6] Z.D. Huang,B. Zhang, S.W. Oh, Q.B. Zheng, X.Y. Lin, N. Yousefi, J.K. Kim, Self-assembled reduced graphene oxide/carbon nanotube thin film as electrodes for supercapacitors, J Mater Chem, 22, 3591–3599, 2012.

[7] N. Yousefi, M.M. Gudarzi, Q.B. Zheng, S.H. Aboutalebi, F. Sharif, J.K. Kim, Self-alignment and high electrical conductivity of

ultralargegrapheneoxide-polyurethane nanocomposites, J. Mater. Chem. 22, 12709-12717, 2012

[8] D. Li, M.B. Muller, S. Gilje, R.B. Kaner, G.G. Wallace, Processable aqueous dispersions of graphene nanosheets, Nat.Nanotechnol, 3, 101-105, 2008.

[9] Z.D. Huang, B. Zhang, R. Liang, Q.B. Zheng, S.W. Oh, X.Y. Lin, N. Yousefi and J.K. Kim, "Effects of Reduction Process andCarbon Nanotube Content on Supercapacitive Performance of Flexible Graphene Oxide Papers"Carbon, 50, 4239-4251, 2012.

[10] A.R. Ranjbartoreh, B. Wang, X. Shen, G. Wang, Advanced mechanical properties of graphene paper, J. Appl. Phys., 109, 014306-6, 2011.

[11] D. A. Dikin, S. Stankovich, , E. J Zimney, R. D. Piner, G. H. B. Dommett, G. Evmenenko, S. T. Nguyen, R. S. Ruoff, Preparation and characterization of graphene Oxide Paper. Nature, 448, 457-460, 2007

[12] S. Park, K. S.Lee, G. Bozoklu, W. Cai, S. B. T. Nguyen, R. S. Ruoff, Graphene Oxide Papers Modified by Divalent Ions—Enhancing Mechanical Properties *via* Chemical Cross-Linking. ACS Nano, 2, 572-578, 2008.

[13] Y. Tian , Y. Cao , Y. Wang , W. Yang , and J. Feng, Realizing Ultrahigh Modulus and High Strength ofMacroscopic Graphene Oxide Papers Through Crosslinkingof Mussel-Inspired Polymers. Adv. Mater. *25*, 2980–2983, 2013

[14] O. C. Compton, S. W. Cranford, K. W. Putz, Z. An, L. C. Brinson, M. J. Buehler, S. T. Nguyen, Tuning the Mechanical Properties of Graphene Oxide Paper and Its Associated Polymer Nanocomposites by Controlling Cooperative Intersheet Hydrogen Bonding. ACS Nano, 6, 2008-2019, 2012

[15] M, Cano, U. Khan, T. Sainsbury, A. O'Neill, Z.M. Wang,I.T. McGovern, W.K. Maser, A.M. Benito, J.N. Coleman. Improving the mechanical properties of graphene oxide basedmaterials by covalent attachment of polymer chains, Carbon, 52, 363-371, 2013

[16] W.O. Lee, J.U. Lee, B.M. Jung, J.H. Byun, J.W. Yi,S.B. Lee, B.S. Kim. Simultaneous enhancement of mechanical,electrical and thermal properties of graphene oxidepaper by embedding dopamine. Carbon, 65, 296-304, 2013

[17] D.A. Dikin, S. Stankovich, E.J. Zimney, R.D, Piner, G.H.B. Dommett, G. Evmenenko, S.T. Nguyen, R.S. Ruoff, Preparation and characterization of graphene oxide paper, Nature, 448, 457-60, 2007.

[18] S. Park, K.S. Lee, G. Bozoklu, W. Cai, S.T. Nguyen, R.S. Ruoff, Graphene oxide papers modified by divalent ions-enhancing mechanical properties via chemical cross-linking, ACS Nano, 2, 572–578, 2008.

[19] A.R. Ranjbartoreh, B. Wang, X. Shen, G. Wang, Advanced mechanical properties of graphene paper, J. Appl. Phys., 109, 014306-6, 2011.

[20] X. Sun, Z. Liu, K. Welsher, J. Robinson, A. Goodwin, S. Zaric, H.J. Dai, Nano-graphene oxide for cellular imaging and drug delivery, Nano Res. 1, 203-212, 2008.

[21] Z. Liu, J.T. Robinson, X.M. Sun, H.J. Dai, Pegylatednano-graphene oxide for delivery of water insoluble cancer drugs, J. Am. Chem. Soc. 130, 10876-10877, 2008.

[22] S.J. Wang, Y. Geng, Q.B. Zheng and J.K. Kim, "Fabrication of highly conducting and transparent graphene films" Carbon 48,1815-1823, 2010

[23] Q.B. Zheng, W.H. Ip, X.Y. Lin, N. Yousefi, K.K. Yeung, J.K. Kim, Transparent conductive films consisting of ultralarge graphene sheets produced by Langmuir-Blodgett assembly, ACS Nano, 5, 6039–6051, 2011.

[24] S. Pan, I.A. Aksay, Factors controlling the size of graphene oxide sheets produced via the graphite oxide route, ACS Nano, 5, 4073-4083, 2011.

[25] X. Wang, H. Bai, G. Shi, Size fractionation of graphene oxide sheets by pH-assisted selective sedimentation, J. Am. Chem. Soc. 133, 6338-6342, 2011

[26] L. Zhang, J. Liang, Y. Huang, Y. Ma, Y. Wang, Y. Chen, Size-controlled synthesis of graphene oxide sheets on a large scale using chemical exfoliation, Carbon, 47, 3365-3380, 2009.

[27] M.M. Waje, X. Wang, W. Li, Y. Yan, Deposition of platinum nanoparticles on organic functionalized carbon nanotubes grown in situ on carbon paper for fuel cells, Nanotechnology, 16, 395-400, 2005

[28] F. Zheng, D.L. Baldwin, L.S. Fifield, N.C. Jr. Anheier, C.L. Aardahl, J.W. Grate, Single-walled carbon nanotube paper as a sorbent for organic vapor preconcentration, Anal Chem, 78, 2442–2446, 2006.

[29] Y. Geng, S.J. Wang, J.K. Kim, Preparation of graphite nanoplatelets and graphene sheets, J. Colloid Interf. Sci. 336, 592-598, 2009

[30] W.S. Hummers, R.E. Offeman, Preparation of graphitic oxide, J. Am. Chem. Soc. 80, 1339, 1958.

[31] S.H. Aboutalebi, M.M. Gudarzi, Q.B. Zheng, J.K. Kim, Spontaneous formation of liquid crystal in ultralarge graphene oxide dispersions, Adv. Funct. Mater, 21, 2978–2988, 2011

[32] X.Y. Lin, X. Shen, Q.B. Zheng, N. Yousefi, L. Ye,Y.W. Mai, J.K. Kim, Fabrication of highly-aligned, conductive, and strong graphene papers using ultralargegraphene oxide sheets, ACS Nano, 6, 10708–10719, 2012.

[33] Standard test for plane strain fracture toughness of metallic materials, ASTM E-399, American

Society for Testing and Materials, Philadelphia, PA, 1987.
[34] A. Gupta, G. Chen, P. Joshi, S. Tadigadapa, P.C. Eklund, Raman scattering from high-frequency phonons in supported n-graphene layer films, Nano Lett. 6, 2667–2673, 2006
[35] A.C. Ferrari, J.C. Meyer, V. Scardaci, C. Casiraghi, M. Lazzeri, F. Mauri, S. Piscance, D. Jiang,K.S. Novoselov, S. Roth, A.K. Geim, Raman spectrum of graphene and graphene layers, Phys. Rev. Lett. 97, 187401- 4, 2006
[36] G. Venugopal, M.H. Jung, M. Suemitsu, S.J. Kim, Fabrication of nanoscale three dimensional graphite stacked junctions by focused-ion-beam and observation of anomalous transport characteristics, Carbon, 49, 2766-2772, 2011.
[37] M.A. Pimenta, G. Dresselhaus, M.S. Dresselhaus, L.G. Cançado, A. Jorio, R. Saito, Studying disorder in graphite-based systems by Raman spectroscopy, Phys. Chem. Chem. Phys. 9, 1276-1291, 2007.
[38] Q.B. Zheng, Y. Geng, S.J. Wang, ZG Li and J.K. Kim, "Effects of functional group on the mechanical and wrinkling properties ofgraphene sheets" Carbon, 48, 4315-4322, 2010.
[39] X.F. Zhang,T.V. Sreekumar,T. LiuandS. Kumar, Properties and structure of nitric acid oxidized single wall carbon nanotube films, J. Phys. Chem. B, 108, 16435-16440, 2004.
[40] J.W. Zhang, D.Z. Jiang, H.X. Peng, F. Qin, Enhanced mechanical and electrical properties of carbon nanotube buckypaper by in situ cross-linking, Carbon, 63, 125-132, 2013
[41] D.F. Caulfield and D.E. Gunderson, Paper testing and strength characteristics, TAPPI proceedings of the 1988 paper preservation symposium: Wahsington, DC, USA. TAPPI Press: pp. 31-40, 1988.
[42] H.W. Greensmith, A.G. Thomas, Rupture of rubber -III Determination of tear properties, Rubber Chem. Technol.29 372-381, 1956.
[43] R.G. Stacer, L.C. Yanyo, F.N. Kelley, Observations on the tearing of elastomers, Rubber Chem. Technol. 58, 421-435, 1985.
[44] Y. Tanaka, H. Abe, T.Kurokawa, H. Furukawa, J.P. Gong, First Observation of Stick-Slip Instability in Tearing of Poly(vinyl alcohol) Gel Sheets, Macromolecules, 42, 5425-5426, 2009.
[45] Seth, R. S. (1996): Optimizing reinforcement pulps by fracture toughness. TappiJ., vol. 79, no 1, pp. 170-178.
[46] D.H. Page and J.M. MacLeod, Fiber strength and its impact on tearstrength. Tappi, J. vol. 75, 172-174, 1992
[47] H. Karlsson, L. Beghello, L. Nilsson, L. Stolpe. Abaca as a reinforcement fibre for softwood pulp, TAPPI J. 6, 25-32, 2007